Robotic Additive Manufacturing system for nuclear industry applications.

Richard French[1], Hector Marin-Reyes[2], Gabriel Kapellmann-Zafra[3], Samantha Abrego-Hernandez[4]

***Abstract*— Increasing industrial demands from the high-value manufacturing industries of quality, productivity, efficiency and security to enable the development of the next generation nuclear power plants has driven the requirement for novel automated and robotic systems. This paper describes the motivation, design and implementation phases of SERFOW (Smart Enabling Robotics driving Free Form Welding), which is an automated welding cell prototype that links the industrial requirements of nuclear manufacturing. Key innovations are found in the integration of a 3D vision system with a robotic manipulator to perform automatic free-form fusion welding for multiple layer material build-up required to expand Additive Manufacturing without human intervention.**

I. INTRODUCTION

The Department of Energy and Climate Change in the UK predicts a 20% electricity demand increase due to demographic and economic growth over the next two decades [1]. Nuclear power is a reliable, cost-competitive and low carbon emission technology that helps to cover the current energy demands. Its usage is expected to increase in parallel with wind and solar technologies to comply with the future predicted power demands [2]. Therefore the importance of the development of smart manufacturing processes that must cope with future nuclear industry demands. European governments are investing in research and development of Additive Manufacturing (AM) processes in the nuclear industry aiming towards zero waste and efficient production of metal products, reducing the cost of the manufactured parts in comparison with the traditional methods [3]. AM is defined as a multi-layer build-up process where the information to build objects is gathered from a three dimensional, 3D, model data [4]. AM has the potential to redefine the manufacturing processes entirely and it is predicted to have significant growth in certain areas. To fully obtain the advantages of AM, new prototypes that reduce the material waste, the number of production steps and the number of distinct parts needed are required to be implemented. These new prototypes have to be autonomous, dynamic, flexible and multi-tooled to perform tasks such as welding and energy directed material deposition AM. This project aims to produce a dynamic free form welding system that is capable of providing low-cost AM. The project will produce an advanced stereo camera system with auto-focus capabilities which can be integrated with a robotic arm and welding power supply. The integrated system will allow the repair and manufacture of high-value aerospace, automotive and nuclear industry components. Gaining flexibility provided by a six-axis robotic arm, the prototype system enables the production of structures using metallic additive filler deposition or to carry out material joining operations when required. By detecting sub-component shape and profile the system assess the addition of material or joint and positions the robotic arm to ensure correct positional accuracy for the AM layers or joining to be conducted. This system is designed to be integrated with different types of welding or AM technologies and is, with further development, capable of working on parts of all shape and sizes autonomously, which is beyond current commercially available systems capabilities. The development of new autonomous AM technologies, as depicted here, adds flexibility and allows for rapid, dynamic adaption of production tasks, reducing the high financial penalties of more complex traditional systems. This is of critical importance to the aerospace, nuclear and petrochemical industries increasingly bespoke parts consist of unique shapes, profiles and sizes. The robotic process will result in direct cost savings for industry, allowing for greater system control during the welding process.

II. METHODOLOGY

Existing methods used in manufacturing require pre-programmed tasks which are inflexible and time-consuming. Procedures are designed for mass production of the same unit component; however, challenges are faced when an updated or a new component is required. These updates are often expensive, due to the need of new jigs and fixtures combined with the set-up time, and increased risk from human error. The prototype system presented in this project emulates the high skills of experienced fusion welding engineers who can manually build-up layers of additive filler wire onto complex shape objects. A representative cooling manifold assembly fabricated from Super Duplex Stainless Steel comprises of a mounting block, connecting tube and an inlet port. This component assembly is used to demonstrate the prototype system fusion joining and a weld build-up (AM) capability as shown in Figure 1. The SERFOW prototype is composed of an extruded aluminium profile chassis structure. Within

This work was supported by Innova UK

[1]Richard French is with the Department of Physics and Astronomy, The University of Sheffield, Sheffield, United Kingdom r.s.french@sheffield.ac.uk

[2]Hector Marin-Reyes is with the Department of Physics and Astronomy, The University of Sheffield, Sheffield, United Kingdom H.Marin-Reyes@sheffield.ac.uk

[3] Gabriel Kapellmann-Zafra is with the Department of Physics and Astronomy, The University of Sheffield, Sheffield, United Kingdom g.kapellmann@sheffield.ac.uk

[4] Samantha Abrego-Hernandez is with the Department of Physics and Astronomy, The University of Sheffield, Sheffield, United Kingdom s.abrego@sheffield.ac.uk

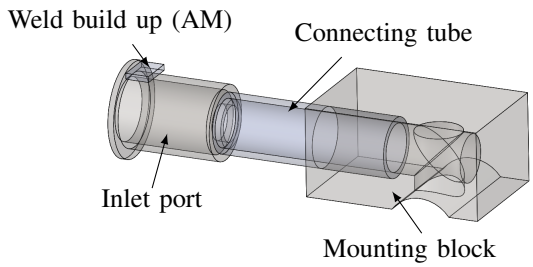

Fig. 1. 3D CAD rendering of the nuclear heat exchanger manifold components.

this structure, the system comprises of a Universal Robots UR-10 six-degrees-of-freedom robot arm combined with a Shadow Robot Smart Grasping System, SGS [5]. The robotic element drives a simple rotary turn-table and is controlled by I3D Robotics (I3DR), stereo vision system Phobos [6] and PosCam. AM and materials joining are conducted by an industry standard TIG welding system. The automatic movements of the welding system (wire feeder and torch) are controlled by two linear motor drives in the "X" and "Z" axis. Figure 2, shows a 3D CAD rendering of the described components when fully assembled during the construction and integration of the system. Work was conducted in the Enabling Sciences for Intelligent Manufacturing Laboratory at the University of Sheffield. The key point about the main structure design was about being able to be flexible and adaptable for future projects.

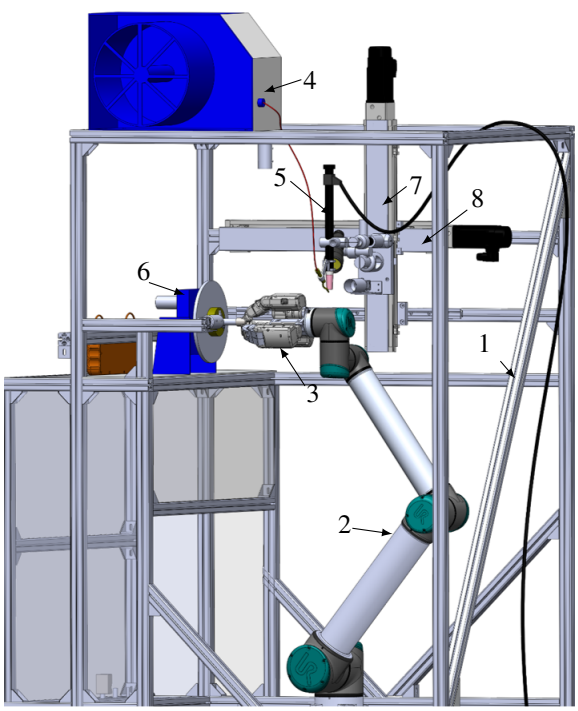

Fig. 2. SERFOW cell: 1) aluminium structure, 2) robotic arm, 3) smart grasper, 4) wire feeder, 5) torch, 6) turn-table, 7) "Z" and 8)"X" linear motor drives.

III. Intelligent welding vision system

A. Project scope

This project aims to develop a 3D vision system that is interfaced with the robotic grasping and welding system. The 3D vision system will acquire the shape, profile and depth information of the objects to undergo manufacturing. Additionally, the vision system confirms grasp, real-time monitoring and feedback to control the welding conditions such as the AM filler wire delivery speed and arc voltage control. Information is delivered to the robot for both trajectories and path planning execution.

B. 3D stereo vision system

The stereo vision produces a 3D model of an object or a target area by matching features between two or more images of the scene. This is known as the correspondence problem and is solved using a stereo matching algorithm [7], [8]. There is an increasing number of published matching algorithms [9], most of which employ some form of correlation between points in the image pairs. Stereo images are usually rectified, such that corresponding features lie on the same pixel line in each image [10]. Stereo vision utilises the fact that 3D points in space project to distinct 2D pixel locations in images of the scene when acquired from two different locations. The differences in pixel coordinates in the images allow reconstruction of the 3D coordinates from the images. Following a calibration process, the stereo algorithm can process the image-pairs to produce a 3D point cloud which is effectively a set of data points where each pixel provides disparity or distance information, of the scene. Figure 3 shows an example of a meshed point cloud where a cylinder can be viewed in a scene.

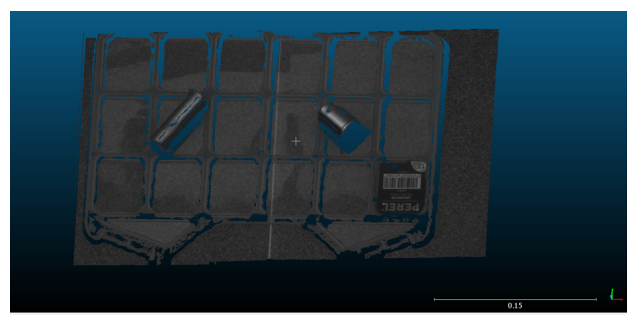

Fig. 3. Example of a point cloud showing a cylindrical object on a flat surface.

The 3D stereo vision system proposed and implemented in this project can be divided into two subsystems: the Phobos and the PosCam. Phobos, is a high-resolution stereo camera developed by I3DR [6]. It can provide a spatial resolution of 0.11 mm, with a depth resolution of 0.45mm at 1m range, over a field of view of 1.06 x 0.88 m. It is used to recognise and obtain the objects dimensional characteristics (profile, shape and depth) in a target scene.

Mounted directly above the loading area, Phobos obtains the positional coordinates of the components to be either

joined or to undergo the AM process. The positional coordinates obtained were used as an input to control the six degrees of freedom UR-10 robot and the smart grasping system. This robotic manipulator located and identified the correct components, grasped the correct component and then loaded it into the automated rotary turn-table. In addition to the camera development, I3DR has also developed the Phobos software which has been integrated and tested in ROS-Industrial [11]. Due to the highly reflective nature of metallic components, illumination problems have been identified during research and development. Therefore, a diffused light method has been produced, using illumination from various angles which were reflected on white surfaces. After the implementation of this method, part detection has been performed and component back-lighting was no longer a problem to the project. It does remain critical for the system to be appropriately set-up to minimise reflections on the component.

The PosCam system is composed of three cameras, A, B and C, model DMK23UM021 positioned in the welding area as Figure 4 shows. Camera A was attached to the welding torch. The centre of this camera was aligned with the welding torch electrode tip. This allowed the precise positioning of the torch tip to the workpiece which was critical to the AM operation or joining by fusion welding.

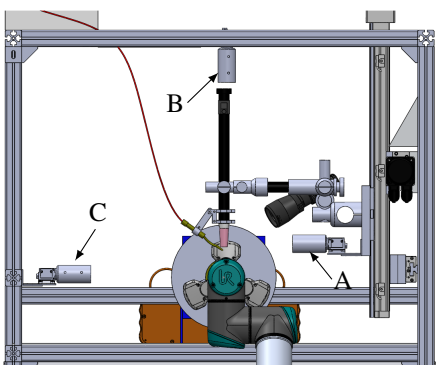

Fig. 4. PosCam system 3D CAD.

Absolute camera precision was determined by the lens choice and working distance. Given that the TIG torch and camera were fixed relative to each other at 150 mm. Therefore, the key parameters became the resolution, field-of-view and depth-of-field at that range. Camera B was mounted vertically on the welding structure and monitored the workpiece position allowing the weld to commence, in conjunction with horizontally mounted camera C. The main purpose of these cameras were to inspect and monitor the welding process from different angles, as shown in Figure 5.

This enabled control over the welding parameters such as voltage, linear welding speed, the distance between arc tip and AM filler wire delivery speed. 3D models of the conducted weld or AM layering were produced and monitored by the stereo vision system to give feedback and make any required modification in the welding parameters as described in [12].

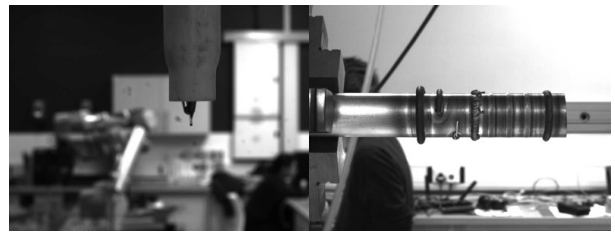

Fig. 5. Left picture acquired by camera A attached to the welding torch, right picture acquired by camera B attached to the aluminium structure.

IV. Smart grasping system

The UR10 robot arm and Shadow SGS were used to pick the correct parts and load them in the correct sequence dictated by the recognition patterns and location of the 3D vision system before final manufacturing. This was a huge advantage over the current manufacturing processes where usually the robot trajectories and grabbing of the pieces must be programmed manually by the line operators.

The main characteristics of the six-degrees-of-freedom UR10 robot arm are the payload mass of 10 kg and the repeatable accuracy of 0.1 mm. The main characteristics of the Shadow SGS are the modularity and flexibility to manipulate different objects sizes, shapes and weights. Various configurations of the design, such as a four-fingered or two-fingered hand were possible. However, in this project, the three-fingered configuration due to the nine-degrees-of-freedom was used as shown in Figure 6. .

Fig. 6. Shadow Robot Smart Grasper system positioning object in a turntable.

V. System interfacing and control

The interfaces and control of SERFOW were designed as shown in Figure 7. The implementation of this design was made with the ROS for LabVIEW software developed by Tufts University [13]. This software has the capability of handling node-to-node transport negotiation and communication using TCP. Its libraries are capable of sending and receiving messages from topics/services, coding or decoding message strings, connecting and turning a device into a ROS master. Once the assembly and the interfacing of the systems

were implemented the steps to perform the welding and AM, were defined as shown in Figure 8.

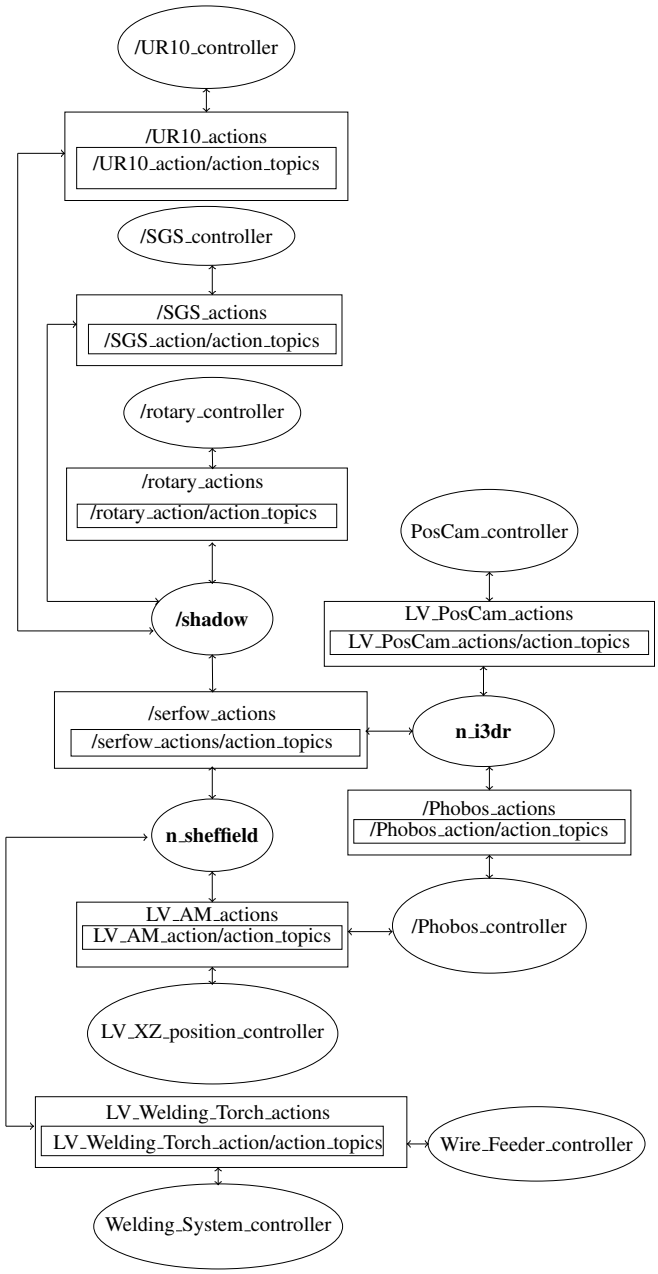

Fig. 7. ROS graph diagram showing nodes and topics to control Serfow system

The fully integrated SERFOW cell including the 3D stereo vision system, the robotic manipulators and the welding system was implemented as shown in Figure 9.

VI. Automated Welding and Additive Manufacturing System

Welding trials on Super Duplex Stainless Steel samples were conducted with a main and background current values of 25 A and 75 A respectively. The welding system used was composed by the Miller Dynasty 350 TIG power source, combined with a TIG torch machine and automatic

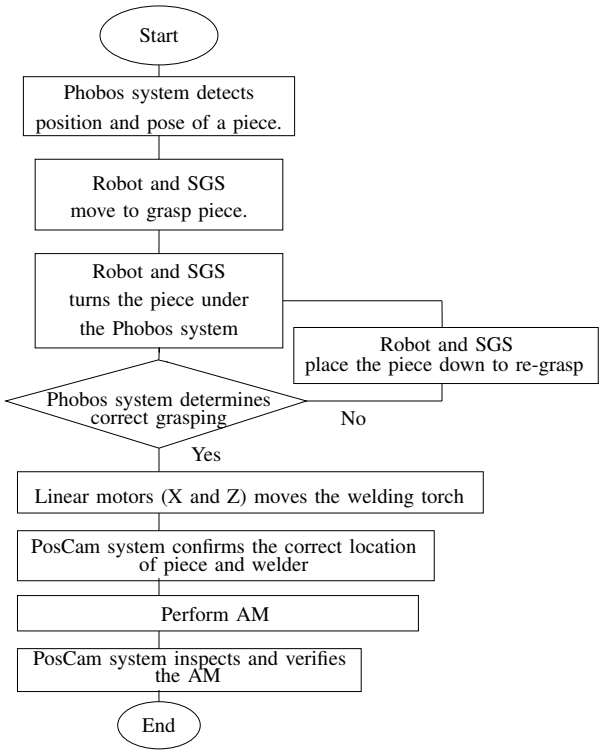

Fig. 8. SERFOW workflow diagram.

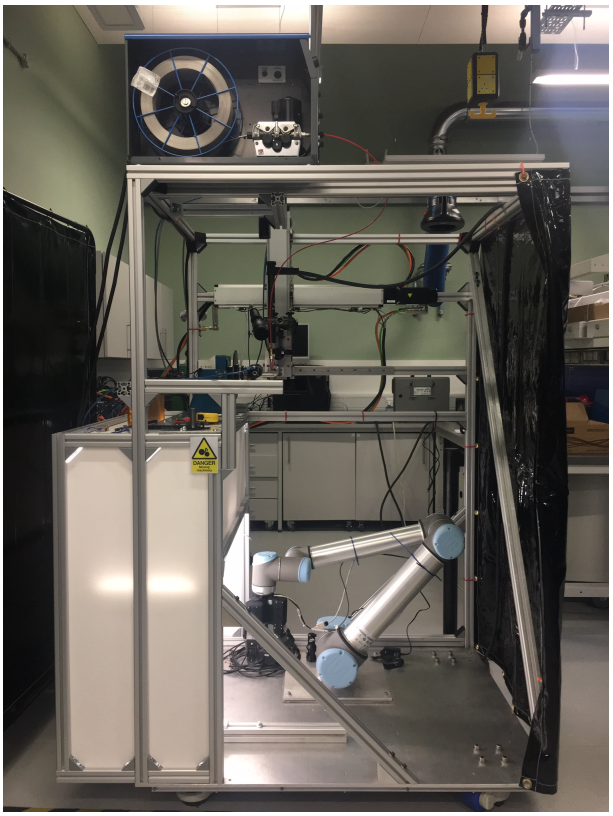

Fig. 9. SERFOW implemented cell.

wire feeder. Layers of weld were applied on a 20mm pipe as shown in Figure 10. Metallographic observations,

temperature, feritscope and tensile test measurements were performed in the welding trials to assess the mechanical properties of the welding.

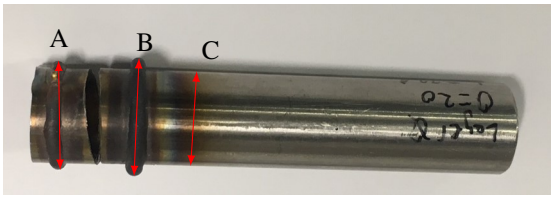

Fig. 10. Welding trials performed in a 20 mm tube where: a) is the first layer of the AM with an outside diameter of 22.5 mm and b) is the second layer of the AM with an outside diameter of 25mm.

A. Metallographic observations

The metallographic observations showed a uniform porosity distribution according to ISO 6520-1:2007)[14], Figure 11. The total area of detected pores covers 0.4% of the weld bead which is below the maximum tolerance of 1% defined by the ISO 5817 [15].

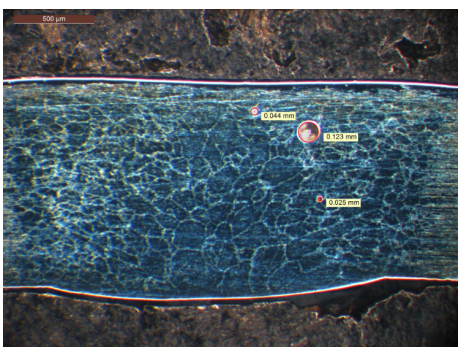

Fig. 11. Metallurgic observations on welding trial 25-75 showing the detail of the weld bead with a magnification value of 50x.

B. Feritscope measurements

The ferrite content affects the mechanical properties, corrosion resistance and weld strength of the materials. In materials such as Super Duplex Stainless Steel, a deficit of the ferrite content reduce the weld strength and increases the development of stress corrosion cracking [16], [17]. Therefore, measurements of the ferrite content have been performed with MP3C FISCHER Feritscope on the 25-75 samples as shown in Table I.

TABLE I
FERRITE CONTENT RESULTS

25/75 sample Ferrite content / %						Average	Std dev
Side 1	41.1	41.2	39.6	39.7	38.8	40.1	0.9
Side 2	40.3	40.9	40.2	40.7	40.1	40.4	0.3
Weld	50.6	49.4	55.8	49.1	50.9	51.2	2.4

The ferrite content found in the Super Duplex Stainless Steel welding trials confirms that ferrite content is greater in the weld (approximately 51.2%) than in the pipe (approximately 40.4%).

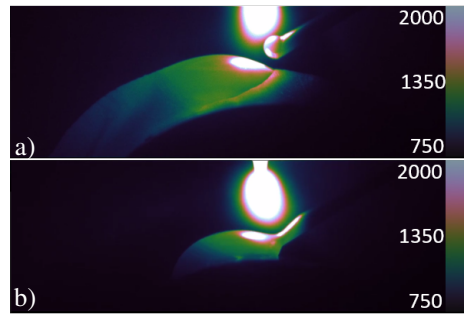

Fig. 12. Temperature measurement of a) 1 layer and b) 2 layers of AM.

C. Temperature measurements

Temperature measurements of 1 layer and two layers of AM were taken with a thermal camera system capable of taking pictures at 80 frames per second with a radiance range from 750°C to 2000°C to quantify the heat transfer as shown in Figure 12. These measurements were useful to determine the durability of the finger-tip of the Shadow SGS and the cooling time of the sample.

D. Tensile test

Tensile tests on the 25-75 welding sample have been performed on a UTS tensile test machine. Elongation has been measured with stroke displacement only as no extensometer could be fitted. Strength has been estimated on the average of the measured diameter and wall thickness of the pipe extremities. The results obtained are shown in Figure 13. The

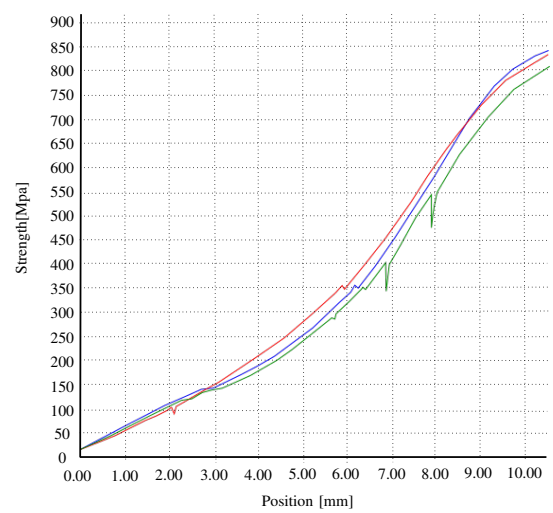

Fig. 13. Tensile test results for 25/75 Super Duplex Stainless Steel welding samples

tensile test performed on the three welding samples broke on the weld. The average Ultimate Tensile Strength (UTS) of the samples was 878 8 MPa. As stated in NFEN 288-3 [18] the UTS should not be less than 800 MPa for UNS S 32750 pipes as stated by in ASTM A789 [19].

VII. CONCLUSIONS AND FUTURE WORK

The fully integrated 3D vision system, UR-10 robot, Shadow SGS and welding system have allowed for successful automation and implementation of materials joining and AM using fusion welding. The designed welding and AM procedure specifications of a main and background current of 25-75 Amps were applied to samples of Super Duplex Stainless Steel which were then subject to evaluation from forms of destructive testing. The metallurgical analysis demonstrates, that whilst the samples which have undergone AM and welding are within an acceptable range according to ISO 5817 ASME A789, there is considerable room for improvement in the reduction of the ferrite count within the weld region or (heat affected zone) HAZ. Now the autonomous welding and AM cell is functioning correctly as an integrated system; future work will be based around the manipulation of the welding or AM specification. By increasing the background current and reducing the main current ratio of the welding power source we expect to be able to see evidence of a considerable reduction in ferrite count around the HAZ.

ACKNOWLEDGMENT

We are very grateful to Ben Crutchley from Industrial 3D Robotics, Fotios Papadopoulos from Shadow Robotics company, Ben Kitchener, Kieren Howarth and Samuel Edwards from the Enabling Sciences for Intelligent Manufacturing Laboratory at the University of Sheffield for their help and their invaluable support.

REFERENCES

[1] N. A. Office, "The department of energy & climate change: Nuclear power in the uk," Website, July 2016, accessed 23 January 2019.

[2] G. Harris, P. Heptonstall, R. Gross, and D. Handley, "Cost estimates for nuclear power in the uk," *Energy Policy*, vol. 62, pp. 431–442, 2013.

[3] T. Wohlers and T. Caffrey, "Additive manufacturing: going mainstream," *Manufacturing Eng*, vol. 151, no. 6, pp. 67–73, 2013.

[4] W. E. Frazier, "Metal additive manufacturing: a review," *Journal of Materials Engineering and Performance*, vol. 23, no. 6, pp. 1917–1928, 2014.

[5] Shadow robotics company ltd, introducing the new modular grasper. [Online]. Available: https://www.shadowrobot.com/products/modular-grasper/

[6] Industrial 3D Robotics, Phobos, url = http://i3drobotics.com/phobos, note= Accessed: 04 January 2019.

[7] E. Mouaddib, J. Batlle, and J. Salvi, "Recent progress in structured light in order to solve the correspondence problem in stereovision," in *Robotics and Automation, 1997. Proceedings., 1997 IEEE International Conference on*, vol. 1. IEEE, 1997, pp. 130–136.

[8] B. Tippetts, D. J. Lee, K. Lillywhite, and J. Archibald, "Review of stereo vision algorithms and their suitability for resource-limited systems," *Journal of Real-Time Image Processing*, vol. 11, no. 1, pp. 5–25, 2016.

[9] R. Bogue, "Robots in the nuclear industry: a review of technologies and applications," *Industrial Robot: An International Journal*, vol. 38, no. 2, pp. 113–118, 2011.

[10] S. Kawatsuma, M. Fukushima, and T. Okada, "Emergency response by robots to fukushima-daiichi accident: summary and lessons learned," *Industrial Robot: An International Journal*, vol. 39, no. 5, pp. 428–435, 2012.

[11] M. Quigley, K. Conley, B. Gerkey, J. Faust, T. Foote, J. Leibs, R. Wheeler, and A. Y. Ng, "Ros: an open-source robot operating system," in *ICRA workshop on open source software*, vol. 3, no. 3.2. Kobe, Japan, 2009, p. 5.

[12] R. French and H. Marin-Reyes, "Underpinning uk high-value manufacturing: development of a robotic re-manufacturing system," in *Emerging Technologies and Factory Automation (ETFA), 2016 IEEE 21st International Conference on*. IEEE, 2016, pp. 1–8.

[13] ROS for LabVIEW by Tufts University, url = www.clearpathrobotics.com/assets/guides/ros/ROSforLabVIEW.html, Accessed: 04 January 2019,.

[14] ISO-6520-1:2007, "Welding and allied processes Classification of geometric imperfections in metallic materials Part 1: Fusion welding," International Organization for Standardization, Tech. Rep., 2007. [Online]. Available: https://www.iso.org/standard/62521.html

[15] ISO-5817, "Welding Fusion-welded joints in steel, nickel, titanium and their alloys (beam welding excluded) Quality levels for imperfections," International Organization for Standardization, Tech. Rep., 2014. [Online]. Available: https://www.iso.org/standard/54952.html

[16] T. Kuroda, K. Ikeuchi, and Y. Kitagawa, "Role of austenite in weld toughness of super duplex stainless steel," *Welding in the World*, vol. 49, no. 5-6, pp. 29–33, 2005.

[17] C. G. Camerini, V. M. A. Silva, I. A. Soares, R. W. F. Santos, J. E. Ramos, J. M. C. Santos, and G. R. Pereira, "Ferrite content meter analysis for delta ferrite evaluation in superduplex stainless steel," *Journal of Materials Research and Technology*, vol. 7, no. 3, pp. 366–370, 2018.

[18] EN288-3:92AMD197, "Specification and approval of welding procedures for metallic materials-welding procedure test for the arc welding of steels," NF EN, Tech. Rep., 2013. [Online]. Available: https://standards.globalspec.com/std/767677/EN%20288-3

[19] ASTM-A789/A789M18, "Standard Specification for Seamless and Welded Ferritic/Austenitic Stainless Steel Tubing for General Service," ASTM International, Tech. Rep., 2018. [Online]. Available: https://www.astm.org/Standards/A789.htm